Charged Particle Spectra in Central S + S Collisions at 200 GeV/c per Nucleon

J. Bächler,[7] J. Bartke,[4] H. Bialkowska,[11] R. Bock,[5] R. Brockmann,[5] P. Buncic,[12] S.I. Chase,[3] I. Derado,[9] V. Eckardt,[9] J. Eschke,[6] D. Ferenc,[12] B. Fleischmann,[5] P. Foka,[5] M. Fuchs,[6] M. Gazdzicki,[6] E. Gladysz,[4] J.W. Harris,[3] W. Heck,[6] M. Hoffmann,[7] P.M. Jacobs,[3] S. Kabana,[6] K. Kadija,[9,12] R. Keidel,[8] J. Kosiec,[10] M. Kowalski,[4] A. Kühmichel,[6] M. Lahanas,[6] J.Y. Lee,[6] A. Ljubicic, Jr.,[12] S. Margetis,[3] R. Morse,[3] E. Nappi,[2] G. Odyniec,[3] G. Paic,[12] A.D. Panagiotu,[1] A. Petridis,[1] A. Piper,[8] F. Posa,[2] A.M. Poskanzer,[3] H.G. Pugh,[3,*] F. Pühlhofer,[8] G. Rai,[3] W. Rauch,[9] R. Renfordt,[6] D. Röhrich,[6] G. Roland,[6] H. Rothard,[6] K. Runge,[7] A. Sandoval,[5] J.J. Schambach,[3] N. Schmitz,[9] E. Schmoetten,[7] I. Schneider,[6] P. Seyboth,[9] J. Seyerlein,[9] E. Skrzypczak,[10] P. Stefanski,[4] R. Stock,[6] H. Ströbele,[6] L. Teitelbaum,[3] M.L. Tincknell,[3] S. Tonse,[3] G. Vasileiadis,[1] G. Vesztergombi,[9] D. Vranic,[12] and S. Wenig[6]

(NA35 Collaboration)

[1] *Department of Physics, University of Athens, Athens, Greece*
[2] *Istituto Nazionale di Fisica Nucleare Sezione di Bari and Politecnico of Bari, Bari, Italy*
[3] *Nuclear Science Division, Lawrence Berkeley Laboratory, Berkeley, California 94720*
[4] *Institute of Nuclear Physics, Cracow, Poland*
[5] *Gesellschaft für Schwerionenforschung, Darmstadt, Germany*
[6] *Department of Physics, Frankfurt University, Frankfurt, Germany*
[7] *Department of Physics, Freiburg University, Freiburg, Germany*
[8] *Department of Physics, Marburg University, Marburg, Germany*
[9] *Max Planck Institute of Physics, Munich, Germany*
[10] *Institute for Experimental Physics, University of Warsaw, Warsaw, Poland*
[11] *Institute for Nuclear Studies, Warsaw, Poland*
[12] *Rudjer Boskovic Institute, Zagreb, Croatia*

(Received 17 June 1993)

The transverse momentum and rapidity distributions of negative hadrons and participant protons have been measured for central $^{32}S + ^{32}S$ collisions at $p_{lab} = 200$ GeV/c per nucleon. The proton mean rapidity shift $\langle \Delta y \rangle \sim 1.6$ and mean transverse momentum $\langle p_T \rangle \sim 0.6$ GeV/c are much higher than in pp or peripheral AA collisions and indicate an increase in the nuclear stopping power. All p_T spectra exhibit similar source temperatures. Including previous results for K^0_S, Λ, and $\overline{\Lambda}$, we account for all important contributions to particle production.

PACS numbers: 25.75.+r

The main objective of the initial experiments in relativistic and ultrarelativistic nucleus-nucleus collisions at the Brookhaven Alternating Gradient Synchrotron (AGS) and the CERN Super Proton Synchrotron (SPS) has been to ascertain whether conditions are favorable for the production and detection of locally deconfined, strongly interacting matter, the quark-gluon plasma. The spectra of produced particles and participant nucleons measured over a broad acceptance in rapidity y and transverse momentum p_T address many questions important to an understanding of the overall reaction dynamics. Most spectral data available [1–3] are from collisions of light projectiles with heavy targets, where it is difficult to disentangle the effects of rescattering in spectator matter from the fundamental participant matter dynamics. In this Letter we present the rapidity and transverse momentum distributions of negatively charged hadrons h^- and participant protons in the target rapidity hemisphere $y < y_{cm}$ (= 3.0) from central $^{32}S + ^{32}S$ collisions at $p_{lab} = 200$ GeV/c per nucleon ($\sqrt{s_{NN}} = 19.4$ GeV). In central collisions of equal-mass nuclei the influence of spectator nucleons is small. We find that the proton mean rapidity shift and mean transverse momentum are higher than in pp or peripheral AA collisions. This indicates that the nuclear stopping power, which is the average inelasticity of the collision, is larger for central S + S collisions.

A ^{32}S beam of momentum $p = 200$ GeV/c per nucleon was extracted from the CERN SPS onto a 1.18 g/cm^2 ^{32}S target. A $2.0 \times 1.2 \times 0.72$ m^3 streamer chamber [4], mounted inside a 1.5 T magnet, measured the trajectories and momenta of charged particles. Forward and midrapidity calorimeters [5] were used for measuring energy flow and triggering the streamer chamber on central collisions. High track density prohibited individual track measurement at forward laboratory angles $\theta_{lab} \lesssim 5°$, limiting the acceptance to $y < y_{cm}$. However, because of the reflection symmetry of the S + S collision system, data from the target hemisphere characterize the reaction dynamics over the full available phase space.

Central events, corresponding to small impact parameters b, are selected either by a transverse energy E_T trig-

ger, which requires large energy deposition in the midrapidity calorimeters, or by a veto trigger, which rejects events with significant energy deposition in the projectile fragmentation domain at forward angles, $\theta_{\rm lab} < 0.3°$. *Minimum bias events* are obtained from a downstream scintillation counter by selecting interactions in which the charge of the projectile changes by more than one unit. *Peripheral events* are chosen from the minimum bias data by also requiring fewer than 100 charged particles in the streamer chamber.

Charged particle trajectories in the streamer chamber were recorded by two independent imaging and data acquisition systems, one employing film cameras [4], the other employing electronic cameras based on charge-coupled devices (CCDs) [6]. The film data set consists of 457 central events from a veto trigger, which selects 2% of the total inelastic cross section $\sigma_{\rm tot} = 1.7$ barns. The CCD data sample comprises 216 events from a less central E_T trigger, which selects 11% of $\sigma_{\rm tot}$. In a geometrical model, these trigger cross sections correspond to $b_{\rm max}$ of 1.0 and 2.5 fm, respectively. The peripheral data set, consisting of 276 film-imaged events, is drawn from the most peripheral 1.0 barns of the minimum bias trigger, which selects 90% of $\sigma_{\rm tot}$. The data sets are summarized in Table I. The h^- data are primarily pions. From our analysis of charged kaon production in S + S collisions [8] we determine the K^- contribution to the h^- data to be (7.6±0.5)% for $p_T \lesssim 1.0$ GeV/c. The proton distributions are deduced from the *charge excess*; for example, $dN/dy\,(AA \to p) = dN/dy\,(AA \to h^+) - dN/dy\,(AA \to h^-)$. This is a good approximation for collisions between isoscalar nuclei.

All data are corrected for geometrical acceptance, for e^+ and e^- misidentified as hadrons, for hadrons resulting from the weak decays of K^0_S and Λ, and for hadrons produced in secondary hadron-nucleus interactions. In addition, the proton data are corrected for the excess of the K^+ over the K^- yield, which has been measured as a function of rapidity in this same experiment [8].

The h^- rapidity distributions are shown in Fig. 1(a) for the veto and E_T triggers. Also shown is the rapidity distribution from minimum bias, isoscalar NN collisions at the same $\sqrt{s}$, obtained by averaging the single-particle inclusive data for $pp \to \pi^\pm X$ and $pn \to \pi^- X$ [9,10]. The shapes of the three distributions are nearly the same. The rms widths assuming symmetry about $y_{\rm cm}$ are 1.22±0.03, 1.24 ± 0.03, and 1.28 ± 0.02 for the veto, E_T, and NN data, respectively. The distributions are too broad to be purely thermal (thermal rms width ≈ 0.6 for any temperature $T \gtrsim m_\pi$). Our data rule out thermal models which incorporate a spherically symmetric radial expansion [11] but are consistent with hydrodynamical models which assume primarily longitudinal expansion [12].

TABLE I. Analyzed data sets. N_{h^-} and N_p are the mean multiplicities of h^- and protons, respectively, for $y < y_{\rm cm}$. $\langle \Delta y \rangle$ is the mean rapidity shift of the participant protons. The N_{h^-} peripheral data are from Ref. [7].

Data set	σ (mb)	N_{h^-}	N_p	$\langle \Delta y \rangle$
Veto	34	46.8 ± 2.5	12.8 ± 1.4	1.58 ± 0.15
E_T	190	35.3 ± 0.6	10.3 ± 1.4	1.58 ± 0.15
Peripheral	1000	9.8 ± 1.0	3.1 ± 0.8	1.00 ± 0.15

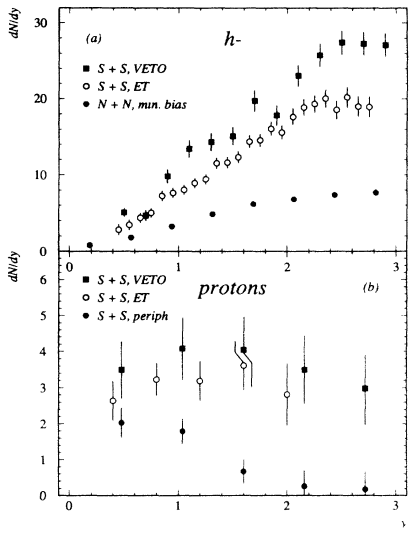

FIG. 1. Event-normalized rapidity distributions for (a) h^- and (b) participant protons. The $N + N$ data in (a) have been multiplied by 10 for ease of comparison.

Figure 1(b) shows the participant proton rapidity distributions for the veto, E_T, and peripheral triggers. The most striking features of the central collision data are the absence of a sharp proton fragmentation peak, which is present in the peripheral trigger data, and the substantially higher participant proton yield at midrapidity. Full stopping in a symmetric AA collision would be indicated by a participant nucleon peak at midrapidity. From Fig. 1(b) the nuclear stopping is clearly incomplete. The data have the same shape for the two central triggers but the integrated yield is higher for the veto trigger. This suggests that for S + S the selection of events with impact parameters smaller than $b \sim 2.5$ fm does not increase the stopping, although it increases the number of participants and enlarges the interaction volume.

To quantify the degree of stopping we calculate the mean rapidity shift $\langle y - y_{\rm \ incident} \rangle$ of *target* nucleons. We find $\langle \Delta y \rangle = 1.58 \pm 0.15$ for both central triggers. This is significantly larger than both what we measure in peripheral S + S collisions, $\langle \Delta y \rangle = 1.00 \pm 0.15$, and what has been estimated for pp collisions from inclusive cross section measurements as a function of Feynman x at fixed p_T, $\langle \Delta y \rangle \approx 1.0$ [13]. However, it is significantly smaller than the $\langle \Delta y \rangle \gtrsim 2$ values observed in central pA collisions at $p_{\rm lab} = 100$ [14] and 200 [15] GeV/c per nucleon with heavy target nuclei. Extrapolations of the S + S results to Pb + Pb predict $\langle \Delta y \rangle_{\rm Pb+Pb} \sim 2$ and $\gtrsim 60$ baryons per unit of rapidity at midrapidity [16]. The

central region will be baryon rich for collisions of heavy nuclei at SPS energies.

The charge-excess method, corrected for the difference in K^+, K^- yields and strange hyperon decays, leads to the number of *observed* participant protons $N_{\rm obs}$. This is an underestimate of the number of participant target protons N_p because of the excitation of nucleons to hyperon states Y. For the veto trigger event sample we derive the correction from the Λ ($\overline{\Lambda}$) and Σ ($\overline{\Sigma}$) yields measured in the same experiment [17] using Wróblewski's empirical rule [18] $N_Y = 1.6(N_\Lambda + N_{\Sigma^0})$. The corresponding correction to the protons in the E_T trigger event sample is obtained by scaling with $N_{\rm obs}$. For the veto and E_T triggers $N_p = 12.8 \pm 1.4$ and 10.3 ± 1.4, respectively, which corresponds to 51 and 41 participant *nucleons* ($4 \times N_p$) per event. The factor 4 accounts for the undetected neutral baryons ($\times 2$) and extends the result to all of phase space ($\times 2$). The mean h^- multiplicity per participant nucleon pair (see Table I) is 3.6 ± 0.5 and 3.4 ± 0.5 for the veto and E_T triggers, respectively, the same within errors as for the peripheral data, 3.2 ± 0.9. It is also the same as the value in *isoscalar NN* collisions at the same energy, 3.2 ± 0.1 [19], determined by isospin averaging the *pp* and *pn* data. This result is surprising in view of the higher stopping power in S + S collisions.

Figures 2(a) and 2(b) show the h^- p_T distributions for the veto and E_T triggers in restricted rapidity intervals. The p_T distributions for the two central trigger data sets have the same shape although the yield

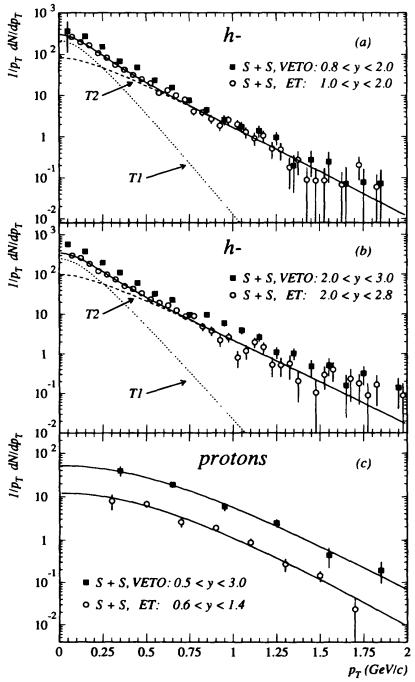

FIG. 2. Event-normalized transverse momentum distributions for (a),(b) h^- and (c) protons. The proton data are reproduced by a simple thermal model. The h^- spectra are overlayed by two-component thermal fits (see text).

is systematically higher for the more central veto trigger. Also shown are two-component thermal model fits $g(p_T) = f(A_1, T_1, p_T) + f(A_2, T_2, p_T)$ of the expression

$$f(A, T, p_T) = A m_\perp K_1(m_\perp/T), \quad (1)$$

where $m_\perp = \sqrt{p_T^2 + m^2}$ is the transverse mass and K_1 is the modified Bessel function. The two-component shape is a natural manifestation of the underlying resonance decay structure [20]. Our data cannot be fitted by any single-temperature function over the full p_T acceptance.

Within statistics, there is no dependence of the p_T distribution on rapidity. The fitted values for T_1, T_2, and $\langle p_T \rangle$ are collected in Table II. Because the fit parameters are correlated we fixed the relative integrated yield in the high-temperature component to $R = 0.6$, the approximate relative π^- yield from direct thermal radiation and ρ decay calculated in Ref. [20] for a hadron resonance gas in thermal and chemical equilibrium. The fitted temperatures of h^- in the different rapidity intervals (see Table II) are the same within errors. This is further evidence that spherically symmetric thermal models do not apply at this energy [21].

The proton p_T distributions are plotted in Fig. 2(c). The different rapidity acceptance of the veto and E_T data accounts for the large difference in yield. The protons can be described by a single-component thermal fit by Eq. (1) which finds $T_p \sim 175$ MeV. Similar temperatures have been obtained from p_T spectra of K^0_S, $K^\pm$, Λ, and $\overline{\Lambda}$ [8, 17]. Unlike the h^-, for which the $\langle p_T \rangle$ is approximately the same as in *pp* collisions near midrapidity [1, 10, 22], for protons $\langle p_T \rangle = (0.622, 0.595) \pm 0.026$ (veto, E_T) GeV/c is significantly higher than in *pp* ($\langle p_T \rangle \approx 0.45$ GeV/c) [10, 23]. This increase is evidence for successive scattering in participant matter, and is consistent with the increase in the stopping power.

The thermal shape of the proton p_T distribution, the two-component structure of the h^- p_T spectra, and the approximate equality $T_p \sim T_2$ can be explained by taking into account resonance sources of final-state charged particles [20, 24]. Most resonances which decay to π^- undergo mass-asymmetric or three-body decays; for example, $\Delta \to N\pi$ or $\eta \to \pi^-\pi^+\pi^0$. The kinematics of both processes focus π^- at low p_T, leading to the two-component structure. Since the proton is the massive

TABLE II. Fits to the h^- and proton p_T distributions. The $\langle p_T \rangle$ is computed for $0.0 < p_T < 2.0$ GeV/c.

Particle	Trigger	T_1 (MeV)	T_2 (MeV)	$\langle p_T \rangle$ (GeV/c)
h^-	Veto	84 ± 21	181 ± 18	0.353 ± 0.006
$1 < y < 2$	E_T	83 ± 6	188 ± 8	0.359 ± 0.006
h^-	Veto	82 ± 10	197 ± 14	0.378 ± 0.006
$2 < y < 3$	E_T	85 ± 11	191 ± 7	0.365 ± 0.006
p	Veto		180 ± 14	0.622 ± 0.026
	E_T		168 ± 10	0.595 ± 0.026

TABLE III. Energy in produced particles, veto trigger.

Particle		Energy (GeV)
π		210 ± 20
η	(π^0 excess only)	6 ± 1
$K\overline{K}$		48 ± 5
$Y\overline{Y}$	(pair production only)	9 ± 1
$N\overline{N}$	(pair production only)	37 ± 22

daughter in the dominant Δ and N^* decay modes, its momentum is strongly correlated with the momentum of its parent and the resonance contribution does not perturb the underlying thermal structure. We conclude that the hadron p_T spectra are thermal with a common temperature $T_f \sim 170 - 190$ MeV. This *spectral* temperature represents the true freezeout temperature only in the absence of radial flow [11].

For the veto trigger, our previous measurements of K^0_S, Λ, and $\overline{\Lambda}$ [17] together with the present data constitute an almost exclusive characterization of central S + S collisions. From the participant proton p_T and rapidity distributions ($0.2 < y < 3.0$) we calculate the average c.m. energy of a participant proton in the final state $E_p = 3.4 \pm 0.14$ GeV. The same procedure applied to the hyperons yields an average c.m. energy of $E_{\rm hyp} = 2.6 \pm 0.3$ GeV. Thus an estimate of the c.m. energy available for particle production is $4N_{\rm obs}(E_i - E_p) + 4N_Y(E_i - E_{\rm hyp}) = 330 \pm 35$ GeV, where E_i is the c.m. bombarding energy. The energy detected in produced particles is summarized in Table III. For the isoscalar S + S collision system we assume $\langle K \rangle = 4\langle K^0_S \rangle$ and $\langle \pi \rangle = 3\langle \pi^- \rangle$. The additional π^0 from three-body η decays are accounted for by assuming an η/π ratio of $\approx 10\%$, consistent with pp data. We assume the charged hyperons have the same energy distribution as the Λ's and a relative abundance of 60%. The number of $N\overline{N}$ pairs is estimated assuming the $\overline{p}/\overline{\Lambda}$ ratio is the same as measured in pp collisions. Note that this choice for the production rate implies that $\overline{N}$ are enhanced by the same factor as the strange particle yield. With these assumptions the 309 ± 30 GeV contained in the produced particles (see Table III) is in good agreement with the energy lost by the 51 participant nucleons.

In summary, the mean rapidity shift and mean transverse momentum of participant protons in central S + S collisions are much higher than in pp or peripheral AA collisions and represent clear evidence of successive scattering and increased, although still incomplete, nuclear stopping. The transverse momentum spectra of all heavy hadrons and the high p_T pions exhibit similar source temperatures. We account for all important contributions to particle production.

We thank the CERN accelerator and experimental area groups and all the NA35 film measuring groups. We thank J. Janesick and the Jet Propulsion Laboratory for help in the CCD camera development. This work was supported by the Bundesministerium für Forschung und Technologie, FRG, the Department of Energy under Contract No. DE-AC03-76SF00098, the Hellenic Secretariat for Research and Technology, the Commission of the European Communities in cooperation with the Ministry for Science of Croatia, and by the Polish Government Research Grant No. 204369101.

* Deceased.
[1] H. Stroebele *et al.*, Z. Phys. C **38**, 89 (1988).
[2] T. Åkesson *et al.*, Z. Phys. C **46**, 361 (1990).
[3] T. Abbot *et al.*, Phys. Rev. Lett. **64**, 847 (1990); J. Barrette *et al.*, Phys. Rev. C **45**, 819 (1992); T. Åkesson *et al.*, Z. Phys. C **53**, 183 (1992).
[4] S. Wenig, Ph.D. thesis, GSI Report No. GSI-90-23, 1990.
[5] J. Bächler *et al.*, Z. Phys. C **52**, 239 (1991).
[6] L. Teitelbaum, LBL Report No. LBL-32812, 1992 (to be published).
[7] J. Bächler *et al.*, Z. Phys. C **51**, 157 (1991).
[8] J. Bächler *et al.*, Z. Phys. C **58**, 367 (1993).
[9] T. Kafka *et al.*, Phys. Rev. D **16**, 1261 (1977).
[10] Y. Eisenberg *et al.*, Nucl. Phys. **B154**, 239 (1979).
[11] K.S. Lee, U. Heinz, and E. Schnedermann, Z. Phys. C **48**, 525 (1990).
[12] J.D. Bjorken, Phys. Rev. D **27**, 140 (1983); L.D. Landau, *Collected Papers* (Pergamon, New York, 1965), p. 569.
[13] W. Busza and A.S. Goldhaber, Phys. Lett. **139B**, 235 (1984).
[14] W.S. Toothacker *et al.*, Phys. Lett. B **197**, 295 (1987).
[15] K. Abe *et al.*, Phys. Lett. B **200**, 266 (1988).
[16] Extrapolations performed using the Lund/FRITIOF nucleus-nucleus simulation for Pb + Pb with parameters, given in Ref. [6], modified to fit the present data.
[17] A. Bamberger *et al.*, Z. Phys. C **43**, 23 (1989); J. Bartke *et al.*, Z. Phys. C **48**, 191 (1990).
[18] A. Wróblewski, Acta Phys. Pol. B **16**, 379 (1985).
[19] M. Gazdzicki and O. Hansen, Nucl. Phys. **A528**, 754 (1991).
[20] J. Sollfrank, P. Koch, and U. Heinz, Phys. Lett. B **252**, 256 (1990).
[21] J. Stachel and P. Braun-Munzinger, Nucl. Phys. **A495**, 393c (1989).
[22] M. Adamus *et al.*, Z. Phys. C **46**, 311 (1988).
[23] B. Alper *et al.*, Nucl. Phys. **B100**, 237 (1975).
[24] G.E. Brown, J. Stachel, and G.M. Welke, Phys. Lett. B **253**, 315 (1991); H.W. Barz, G. Bertsch, D. Kusnezov, and H. Schulz, Phys. Lett. B **254**, 332 (1991).